Results in Materials 2 (2019) 100022

Contents lists available at ScienceDirect

Results in Materials

journal homepage: www.journals.elsevier.com/results-in-materials

Determining Young's modulus of coatings in vibrating reed experiments using irregularly shaped specimens

Nils Rösemann, Torben Fiedler *, Hans-Rainer Sinning, Martin Bäker

Technische Universität Braunschweig, Institute of Materials, Langer Kamp 8, 38106, Braunschweig, Germany

ARTICLE INFO

Keywords:
Vibrating reed
Young's modulus
Gas flow sputtering
HVOF
Yttria stabilized zirconia
NiCrAlY

ABSTRACT

Knowing Young's modulus of coatings is important to understand the stress evolution and failure of coating systems. However, such values are often not available for modern coatings and/or cannot be determined by existing methods for attaining a global stiffness. In this paper, a new method is described and validated that can be used even for brittle, highly porous, and irregularly shaped coatings, for example sputtered or thermally sprayed thermal barrier coatings: In vibrating reed experiments, the resonance frequencies of the specimens are determined. The specimen geometry is measured by a computer tomograph, and a finite element simulation based on that measured geometry is carried out to determine Young's modulus. To validate this method, a monocrystalline irregularly shaped silicon plate with known Young's modulus was measured. The method is tested on different metallic thermal spray coatings, for which other mechanical test methods for Young's modulus were also applicable for comparison. Lastly, a very porous, gas flow sputtered zirconia thermal barrier coating was analyzed where other methods were not suitable.

1. Introduction

The mechanical behaviour of coatings is determined by their mechanical properties that are often difficult to measure. Young's modulus is especially important because it determines the stresses in a coating that is subjected to strains imposed by the substrate. For example, spallation or vertical cracking in thermal barrier coatings is often driven by the stored strain energy which scales linearly with the in-plane Young's modulus [1]. Finite element modelling of the failure mechanisms can help to predict the lifetime of thermal barrier coatings [2–7], but requires accurate materials data like the effective Young's moduli of the different components of the coating system.

Young's moduli of coatings can be measured by various techniques, each with their own merits and drawbacks. Often, different measurement methods can lead to large differences of the measured values due to differences of the applied stress during the tests, especially in ceramic coatings [8,9], or due to the different probing volume [10].

Widely used and easy to implement are indentation tests, where a relatively small fraction of the specimen volume is tested (small indenter size coupled with low force). The resulting Young's moduli can approach the value of the bulk material [8] because pores, microcracks, splat or column boundaries, oxide lamellae (in metallic coatings) and other defects cannot be registered [10]. Therefore, a "local stiffness" is usually obtained by indentation [11]. In addition, measured values often exhibit a high scattering [10,12].

A more global in-plane stiffness can be derived from cantilever-as well as three- or four-point flexural bending tests (e.g. Refs. [9–11,13,14]), provided the tested specimen volume is beyond the length scale of the microstructural features. In that case, the whole composite consisting of coating material, pores, splat- or column boundaries, and oxides is measured, and the derived "effective" Young's moduli can be significantly lower compared to indentation results. To acquire exact results for the coating from these static methods, testing of free-standing coatings is beneficial. Nevertheless, it is not always possible to detach a coating and retain its desired rectangular shape to determine its Young's modulus analytically [12].

Besides these static mechanical test methods, the dynamic impulse excitation technique (IET) has become popular as a fast and easy, non-destructive resonance technique [1,15–18], using oscillations of the specimen that are induced by a single impact and recorded by a microphone [15]. It has been shown by Paul [1] that the derived stiffness values are in good agreement with the results from static flexural bending tests. However, usual IET measurements are not well suited for too small or fragile samples.

* Corresponding author.
E-mail address: t.fiedler@tu-braunschweig.de (T. Fiedler).

https://doi.org/10.1016/j.rinma.2019.100022
Received in revised form 21 August 2019; Accepted 3 September 2019
Available online 10 September 2019

Another resonance technique is the vibrating reed (VR) technique where, different from IET, a sinusoidal excitation is used to select only one single, specific vibration mode. By measuring damping and resonance frequency of this (usually flexural) vibration, both the internal friction and Young's modulus of the studied material can be determined [19–24].

The most common method to investigate coatings in these dynamic experiments is to measure both coated and uncoated specimens and calculate Young's moduli analytically by comparing the resonance frequencies (for example in Refs. [22,23]). Although this method is applicable for thin films with a constant thickness and a negligible interface roughness, it is not suitable for coatings with a large surface or interface roughness or coatings whose effective stiffness is some orders of magnitude below that of the substrate. Furthermore, residual stresses or a curvature of the coated samples may be problematic for the accurate calculation of Young's modulus [22]. Thus, free standing coatings may be used here as well. For ideal flat parallelepiped coating specimens, Young's moduli can then be calculated analytically [25], while complex geometries like irregularly shaped fragments or coatings with a high surface roughness require a numerical approach.

It is the scope of this paper to demonstrate how the vibrating reed experiment can be used to derive an in-plane Young's modulus even with irregularly shaped specimens. To measure these complex geometries, computer tomography is combined with finite element simulations to calculate the relation between measured resonant frequencies and Young's modulus.

The method is first validated using a monocrystalline silicon plate with known Young's modulus and afterwards applied to metallic HVOF coatings and gas flow sputtered zirconia coatings. The metallic HVOF coatings are currently investigated as a protective coating for the inside of liquid rocket combustion chambers [26,27]. To elucidate the failure mechanisms of these coatings and to predict the coatings' lifetime, finite element simulations are carried out [28,29]. For these simulations it is important to determine the material properties even at high temperatures. For Young's modulus, this can be done with vibrating reed tests, where the main benefit is that only one sample is needed to cover a wide temperature range, as reported previously in Ref. [30]. The main purpose of the present work is to compare the vibrating reed technique to other measurement methods. Thus, compression and tensile tests were conducted at room temperature on free-standing coatings. At higher temperatures, these tests would have been affected by creep, whereas only a small influence of creep should be expected in the vibrating reed due to the high frequencies and small oscillation amplitudes.

Finally, gas flow sputtered zirconia coatings are tested. These coatings were recently developed to investigate an alternative deposition technique for thermal barrier coatings with a focus on the desired columnar microstructure, but without the need of high vacuum [31–34]. Due to this columnar microstructure and the relatively high porosity (over 50%) and brittleness, common measurement methods for Young's modulus were not successful so far: indentation tests would lead to an overestimation of the stiffness [8] due to the compression of the columnar microstructure and crack closure. Other methods like flexural bending tests were not applicable because free standing samples with the desired size and rectangular shape could not be fabricated. Furthermore, some methods require a relatively large deflection of the samples, which would lead to a cracking of the coatings along the column boundaries. In this work, it is shown that the vibrating reed technique is suitable to measure Young's modulus of these coatings. It is expected that the small bending amplitudes during vibration will not damage the samples.

2. Experimental details

2.1. The vibrating reed apparatus

The vibrating reed measurements were carried out in a vacuum apparatus equipped with a Bordoni-type [35] capacitive system that uses the same electrode for both exciting and detecting the resonance vibrations (see Refs. [19–21] for more details). Such a single-electrode system, together with its special design in the current vibrating reed apparatus, gives maximum flexibility for sample shape and size down to very small dimensions (at minimum about a few mm in length, 0.5 mm in width and 10 μm in thickness, respectively). In the present case, flat samples of different dimensions, as specified in detail below, were clamped at one end in a stiff mounting device and electrostatically excited at the free end. With very small strain amplitudes (typically of the order 10^{-6}), eigenfrequencies of the vibrating specimen can be detected in a range between about 10^2 s^{-1} and $2 \cdot 10^4$ s^{-1}.

2.2. Preparation of the samples

Three different types of samples were used in this study: Vibrating reed samples, tensile samples and compression samples. The preparation of these samples is described in the following.

The silicon vibrating reed sample for the reference experiment was cut out of a monocrystalline silicon wafer by cracking in a way that the longitudinal axis as well as the normal of the sample were in the {100} crystallographic directions. The irregularly shaped sample had a length of 33 mm, a thickness of 0.65 mm and a mean width of approximately 4 mm. The silicon sample is shown in Fig. 1.

The metallic coatings investigated in this study were applied with high velocity oxyfuel spray, details on the coating process can be found in Ref. [30]. Three coatings were measured in the present study: a state of the art NiCrAlY bond-coat as well as a "Rene80" nickel-based superalloy coating and a newly developed NiCuCrAl [37] coating. The composition of the NiCrAlY was Ni-Cr22-Al20-Y1 (all compositions are weight-%), the composition of the Rene80 alloy was Ni-Cr14-Co9.5-Ti5-Mo4-W4-Al3, and the composition of the NiCuCrAl coating was Ni-Cu30-Al6-Cr5. For the vibrating reed experiments, coatings with a thickness of approximately 2 mm were applied on aluminium substrates that were removed subsequently in a 20 wt.-% to 25 wt.-% dilute NaOH solution. From these free standing coatings, slices with a thickness of 50 μm–200 μm (depending on the minimum producible thickness for the different materials), a width of approximately 2 mm and a length of 15 mm–25 mm were cut with a low speed precision saw. Excluding the part of the sample mount, the resulting length of the vibrating reeds was 10 mm–20 mm.

For tensile tests on the metallic coatings, flat tensile specimens according to DIN 50,125 (Shape H) with a thickness of 0.5 mm–1 mm were used, compression tests were performed on hollow cylindrical samples with an inner diameter of 10 mm, a height of 20 mm and a wall thickness of approximately 0.6 mm. Both, the tensile and the compression tests, were conducted on free standing coatings. The cross-sectional area for the determination of the stress was measured with the image-analysis software of an Olympus optical microscope. For more details of the tensile and compression tests, see Ref. [30].

For determining Young's modulus of irregular, highly porous zirconia

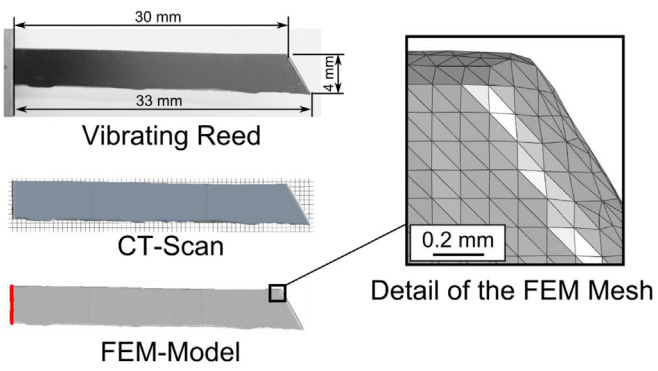

Fig. 1. Example of the geometry and the FEM-mesh of the silicon vibrating reed sample.

coatings, a 150 μm thick coating of partially stabilized zirconia coating (4 at.-% yttria) is applied by a reactive sputter process, the Gas Flow Sputtering (GFS) technique, on a polished FeCrAlY substrate. The GFS process is characterized by an intensive hollow cathode glow discharge and an argon gas-flow-based material transport at fine vacuum pressures. For the target, a Zr-7.6Y (at.-%) alloy is used. The sputtered material is oxidized by reactive-gas (pure oxygen). For a detailed description of the process see for example [31–34], a micrograph of the coating structure is shown in the supplementary material. A free-standing coating is produced by dissolving the substrate in a commercial V2A mordant (containing hydrochloric and nitric acid) at a temperature of 55 °C. Cutting the samples into the desired shape of approximately 3 mm × 10 mm prior to this process (in contrast to cutting the free-standing coating) minimizes the occurrence of unwanted cracks in the brittle coating.

The nonmetallic silicon and yttria coatings had to be coated with a thin gold layer prior to the vibrating reed measurements, to ensure sufficient electric conductivity for the capacitive excitation-detection system. The metallic coatings could be excited electrostatically without further treatment.

2.3. Determination of Young's modulus from the eigenfrequencies

2.3.1. Analytical approach for rectangular specimens

The eigenfrequencies of the vibrating reed are proportional to the square root of the flexural rigidity [25], thus they are proportional to the square root of Young's modulus in case of a homogeneous material. The constant of proportionality depends on the sample's density and the vibration mode, and can be calculated analytically for samples with a simple geometry. For flat parallelepiped shaped geometries, the relation between the flexural vibration frequency, f, at mode i and Young's modulus, E, can be expressed by the following equation [25] (using classical Euler-Bernoulli beam theory that provides reasonable approximations for slender beams with about $l/d > 30$ [38]):

$$f_i = \frac{\alpha_i^2}{4\pi\sqrt{3}} \cdot \frac{d}{l^2} \cdot \sqrt{\frac{E}{\rho}} \tag{1}$$

d is the thickness and l is the free length of the specimen, ρ is the mass density, and α_i is the solution of the following frequency equation:

$$cos\alpha_i \cdot cosh\alpha_i = -1 \tag{2}$$

Besides the flexural vibration, a torsional vibration is also possible. This is not considered here, since the analytical approach is difficult [22] and most of the excited frequencies in the experiments came from flexural vibration.

2.3.2. Numerical approach for irregularly shaped specimen

For vibrating reed specimens with complex geometries, the flexural rigidity cannot be calculated analytically, and equation (1) is not valid anymore. Thus, to determine the relation between the frequency and Young's modulus for the vibrating reed specimens even with complex geometries, finite-element (FE) simulations were carried out. The geometry of the specimens was measured in a computer tomograph (nanotom s, General Electric) and exported via the STL interface. The geometry was then meshed with the tetrahedral mesh generator TetGen [39] and imported in Abaqus Standard [40]. 3D modified tetrahedral second order stress/displacement elements with a high mesh density with edge lengths of ≈0.1 mm were used, resulting in meshes with 100,000 to 250,000 elements, depending on the size of the sample. A mesh convergence study was performed to ensure that the mesh density was sufficiently large. The geometry of the sample, the CT scan, the FEM model and the mesh are exemplified in Fig. 1. The clamped part of the vibrating reed was fixed by a displacement boundary condition (left end in Fig. 1).

Three material parameters are required to calculate the frequency: density, Poisson's ratio and Young's modulus. The density was taken from measurements as described below. A reasonable estimate for Poisson's ratio was made; as shown below, this has only a minor influence on the final result. The eigenfrequencies were then calculated with an initial guess for Young's modulus using a frequency step. Since those frequencies are proportional to the square root of Young's modulus (see section 2.3), the proportionality factor was used to calculate the Young's modulus of the vibrating reed specimens from the experimental resonance frequencies. To validate this procedure, the calculated Young's modulus was used in one simulation to re-calculate the frequencies. As expected, due to the linearity of the problem, the re-calculated frequencies agreed perfectly with the expected values.

The sample holders had to be machined from aluminum to be X-ray transparent for the CT measurements (see supplementary material). If the use of these sample holders is not possible, another way of sufficiently precise implementation of the present numerical approach is offered by partially notched samples, as originally developed for internal friction measurements [41]. Such notched samples possess a second, anti-phase vibration mode whose resonance frequency is rather insensitive to the exact clamping position, so that the clamped length for the above displacement boundary condition may be measured just by a simple scale rule, and the CT scan may then be carried out on the unmounted sample without the need to identify the exact position of the mount. However, as some of the present coatings were too brittle for cutting the notches, such notched samples were not used here, and details are to be given elsewhere.

Poisson's ratio for the FEM simulations of the metallic coatings was assumed to be 0.3, according to measurements by Taylor et al. [42] on CoNiCrAlY coatings. For the zirconia coatings, a Poisson ratio of also 0.3 was assumed. To test the influence of the Poisson ratio, simulations with values of 0.0 and 0.4 were carried out exemplarily on one sample. The elastic constants of silicon for the simulation of the reference experiment were taken from the literature [43].

For silicon, a density of 2.336 g/cm^3 [44] was used for the FEM simulations. The density of the metallic coatings was measured previously on coatings from the same batch as used in the present study [30] and is 7.7 g/cm^3 for NiCuCrAl, 7.2 g/cm^3 for NiCrAlY, and 7.9 g/cm^3 for Rene80. The density of the zirconia coatings was 2.1 g/cm^3, obtained from weight measurements with a microbalance and volumetric measurements with a computer tomograph.

3. Results and discussions

3.1. Young's modulus of monocrystalline (100) silicon

To test the accuracy of the FEM modelling, monocrystalline silicon wafers were used as a reference material, as described in detail in the preceding section. The elastic constants of the silicon sample were taken from Ref. [43] (see supplementary material), and the simulated frequency was compared to the actual frequency of the corresponding measurement. For the first mode of the non-rectangular sample shown in Fig. 1, the frequency from the simulations was 804 s^{-1}, whereas the measured frequency was 801 s^{-1}. For the second mode, the simulation shows a frequency of 4984 s^{-1}, and the measured frequency was 5002 s^{-1}. Higher modes were not reliably measurable anymore in the apparatus due to the high frequencies.

The maximum difference between simulation and experiment is about 0.4% and may be caused by measurement uncertainties especially by determining the shape of the samples in the computer tomography. Furthermore, the samples were assumed to be fixed in a rigid mounting, whereas in reality, the sample mount has a finite stiffness. This may result in a small deviation between the measured frequency and the simulated frequency of the model with a rigid mount. Anyway, the small difference between experiment and simulation shows the reliability of the measurement method in this paper.

3.2. Young's moduli of thermally sprayed metallic coatings

To investigate the accuracy and comparability of the measurements, Young's moduli of HVOF-sprayed metallic coatings were compared to compression and tensile tests on free-standing coatings.

Young's modulus of the NiCrAlY coating (Fig. 2) measured with vibrating reed is 124 GPa, which is in good agreement with the values from the tensile tests where 120 ± 3 GPa has been measured on 5 samples. Data from compression tests are not available for the NiCrAlY coating.

In case of the Rene80 coating (Fig. 3), Young's modulus obtained from vibrating reed is 165 GPa and lies within the range of the error bars from the compression tests, where the measured value is 154 ± 19 GPa (measured on 4 samples). The tensile tests lead to the same average of 154 GPa; due to the small batch size of 2 samples no error bars are shown here, but these values are scattering similar to those from the compression tests.

Young's modulus of the NiCuCrAl coating (Fig. 4) measured with vibrating reed is 132 GPa, similar to the values of 134 ± 8 GPa (4 samples) measured in the compression tests. A Young's modulus of 146 ± 11 GPa (measured on 10 samples) was found in the tensile tests.

The maximum difference of Young's moduli between the vibrating reed technique and tensile- or compression test in the present study on metallic HVOF coatings is 11%, the average difference is even lower. In most cases, this difference is negligible compared to the large scattering of the values within a single test method. In the literature, even larger differences between different testing methods have been reported: for example, Margadant et al. [10] carried out extensive measurements of Young's modulus of vacuum plasma sprayed NiCrAlY coatings with dynamic mechanical analysis, supersonic measurement methods and four-point flexural bending tests, where a maximum difference of 18% between the moduli measured with different methods was observed. This difference has been explained by the different probing volumes in the different tests, which result in different influences of defects, splat boundaries, coating- or interface roughness, or even of the underlying substrate.

3.3. Young's modulus of irregular, highly porous ceramic thermal barrier coatings

To determine Young's modulus of a ceramic thermal barrier coating, the resonance frequencies of six specimens were measured and evaluated

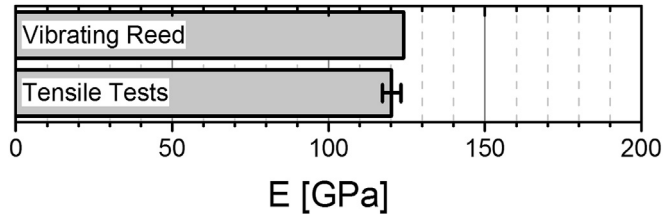

Fig. 2. Young's modulus of the NiCrAlY coating.

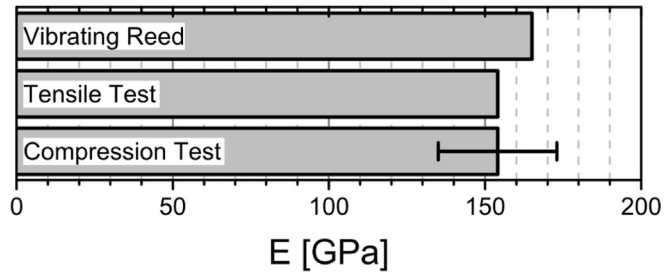

Fig. 3. Young's modulus of the Rene80 coating.

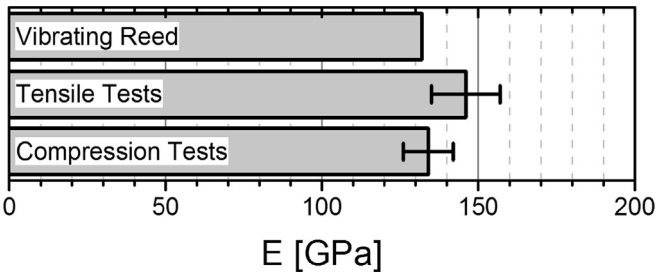

Fig. 4. Young's modulus of the NiCuCrAl coating.

according to section 2. The resulting Young's moduli are presented in Fig. 5. It was possible to excite at least three resonance frequencies per specimen. Therefore, at least three data points for Young's modulus can be drawn, providing a basis for verification. Generally, all determined data points are in the range between 1.2 GPa and 1.5 GPa. Less scattering was observed for the Young's moduli of specimens 1 and 5 where all measured values were within 50 MPa. The scattering of the other specimens was a bit higher, but still in the range of 10%, which may be caused by microcracks. The influence of the microcracks can change with the vibration mode: In vicinity of a node where the bending momentum approaches zero, the influence of a crack is negligible. Whereas in regions with a larger bending momentum, cracks may lead to a reduction of the sample's stiffness and to an underestimation of the calculated young's modulus. Thus, different vibration modes may lead to different calculated Young's moduli when critical microcracks are present.

Since no reliable values for Poisson's ratio were available, a value of 0.3 was assumed in the simulations (see section 2). To test the influence of possible errors in the Poisson ratio ν, simulations with $\nu = 0.0$ and $\nu = 0.4$ were carried out additionally for sample 2: the resulting Young's moduli determined on the mode 1 flexural vibration were 1.25 GPa for $\nu = 0.0$, and 1.23 GPa for $\nu = 0.4$, the maximum difference from the value obtained with the assumed Poisson's ratio of $\nu = 0.3$ (1.23 GPa, see Fig. 5) was 0.02 GPa (2%). Only at higher modes, a maximum difference of 0.12 GPa (10%) to the value determined with $\nu = 0.3$ was determined. The mean Young's moduli averaged over all 4 vibration modes differed by just 0.07 GPa (5%). This difference is still in the range of the overall scattering of the measurement results. Extreme values were chosen for the variation of the Poisson ratio; thus it can be expected that the influence of uncertainties in ν to the measurement results are even smaller and somehow negligible.

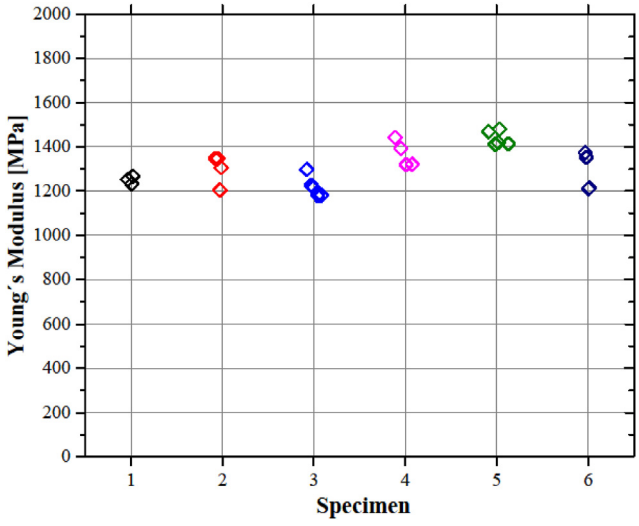

Fig. 5. Derived Young's modulus for a GFS thermal barrier coating. For each specimen, each measured eigenfrequency provides one data point.

Since there are no other Young's moduli for gas flow sputtered zirconia coatings in the literature, its magnitude is compared to two established deposition techniques, atmospheric plasma spraying (APS) and electron beam – physical vapor deposition (EB-PVD). The apparent Young's modulus of zirconia coatings can be as low as several GPa if measured by flexural bending tests (APS [11,13,45]; EB-PVD [46]), but can also exceed 100 GPa if measured with indentation APS [11,47]; EB-PVD [48–50]). It has to be noted that young's modulus of these ceramic coatings is highly dependent on the magnitude of the applied stress, and compressive loads for example in indentation tests lead to an overestimation of Young's modulus [8,9]. Furthermore, indentation tests represent a small probing volume, whereas other measurement techniques like flexural bending tests consider a global stiffness of the whole coating including voids and pores. Thus, the measured (apparent) Young's moduli from the vibrating reed experiment can be better compared to the stiffness values of the flexural bending test. Furthermore, we expect the GFS coatings to exhibit a lower stiffness than the conventionally processed coatings because of the columnar microstructure and the high porosity of over 50%. Therefore, the determined values seem plausible and prove that the combined test setup of vibrating reed apparatus, computer tomograph and finite element simulation can be used to analyze irregularly shaped specimens where other methods fail.

4. Conclusion

A new method to determine Young's modulus has been described, validated with monocrystalline silicon and applied for three metallic and one ceramic thermal barrier coating:

- The resonance frequencies of the specimen are determined in a vibrating reed measurement. The specimen's volume is imaged by a computer tomograph, and a finite element simulation based on the before determined specimen volume is carried out to determine the Young's modulus.
- In a validation experiment with a monocrystalline silicon specimen with known Young's modulus, it has been shown that Young's modulus can be determined reliably.
- Thermally sprayed metallic coatings were tested in the vibrating reed experiments. The resulting Young's modulus is compared to values from tensile and compression tests, and a maximum deviation of 11% between these measurements was found. This deviation is in the range of the scattering of the results in the tensile and compression test, and even lower than reported in the literature for similar coatings with other measurement methods.
- The apparent Young's modulus of a highly porous, gas flow sputtered zirconia coating could be determined to be in the range of 1.2 GPa–1.5 GPa where other methods are unsuited to determine a global stiffness.
- It is not necessary to determine an exact value of the Poisson ratio for reliable measurement results.

Concluding, this new method is able to determine Young's modulus of even irregularly shaped thin specimens like coatings. Especially, if flexural bending tests or supersonic measurement methods are not available or impracticable and a more global stiffness than derived from indentation tests is needed, the vibrating reed measurement will be a feasible alternative. Furthermore the method is not limited to coatings, but can be used for all kind of small and thin samples, for example biomaterials [51].

Acknowledgments

The authors gratefully acknowledge the support by the German Research Foundation and the Open Access Publication Funds of the Technische Universität Braunschweig, the financial support by the German Research Foundation (DFG), contract No. Ba 1795/12-1, and DFG Sonderforschungsbereich Transregio 40, project D2.

Appendix A. Supplementary data

Supplementary data to this article can be found online at https://doi.org/10.1016/j.rinma.2019.100022.

References

[1] S. Paul, Stiffness of plasma sprayed thermal barrier coatings, Coatings 7 (2017) 68.
[2] S. Wei, W. Fu-chi, F. Qun-bo, M. Zhuang, Lifetime prediction of plasma-sprayed thermal barrier coating systems, Surf. Coat. Technol. 217 (2013) 39–45.
[3] R. Vaßen, S. Giesen, D. Stöver, Lifetime of plasma-sprayed thermal barrier coatings: comparison of numerical and experimental results, J. Therm. Spray Technol. 18 (2009) 835.
[4] E.P. Busso, Z.Q. Qian, M.P. Taylor, H.E. Evans, The influence of bondcoat and topcoat mechanical properties on stress development in thermal barrier coating systems, Acta Mater. 57 (2009) 2349–2361.
[5] M. Bäker, J. Rösler, G. Heinze, A parametric study of the stress state of thermal barrier coatings Part II: cooling stresses, Acta Mater. 53 (2005) 469–476.
[6] M. Bäker, P. Seiler, A guide to finite element simulations of thermal barrier coatings, J. Therm. Spray Technol. 26 (2017) 1146–1160.
[7] J. Rösler, M. Bäker, K. Aufzug, A parametric study of the stress state of thermal barrier coatings- Part I: creep relaxation, Acta Mater. 52 (2004) 4809–4817.
[8] J. Malzbender, R.W. Steinbrech, Determination of the stress-dependent stiffness of plasma-sprayed thermal barrier coatings using depth-sensitive indentation, J. Mater. Res. 18 (2003) 1975–1984.
[9] T. Wakui, J. Malzbender, R.W. Steinbrech, Strain analysis of plasma sprayed thermal barrier coatings under mechanical stress, J. Therm. Spray Technol. 13 (3) (2004) 390–395.
[10] N. Margadant, J. Neuenschwander, S. Stauss, H. Kaps, A. Kulkarni, J. Matejicek, G. Rössler, Impact of probing volume from different mechanical measurement methods on elastic properties of thermal sprayed Ni-based coatings on a mesoscopic scale, Surf. Coat. Technol. 200 (2006) 2805–2820.
[11] J.A. Thompson, T.W. Clyne, The effect of heat treatment on the stiffness of zirconia top coats in plasma-sprayed TBCs, Acta Mater. 49 (2001) 1565–1575.
[12] W. Tillmann, U. Selvadurai, W. Luo, Measurement of the young's modulus of thermal spray coatings by means of several methods, J. Therm. Spray Technol. 22 (2013) 290–298.
[13] D. Schwingel, R. Taylor, T. Haubold, J. Wigren, C. Gualco, Mechanical and thermophysical properties of thick PYSZ thermal barrier coatings: correlation with microstructure and spraying parameters, Surf. Coat. Technol. 108–109 (1998) 99–106.
[14] C. Lyphout, A. Fasth, P. Nylen, Mechanical property of HVOF inconel 718 coating for aeronautic repair, J. Therm. Spray Technol. 23 (2014) 380–388.
[15] M. Alfano, L. Pagnotta, Measurement of the dynamic elastic properties of a thin coating, Rev. Sci. Instrum. 77 (2006), 056107.
[16] M.F. Slim, A. Alhussein, A. Billard, F. Sanchette, M. François, On the determination of Young's modulus of thin films with impulse excitation technique, J. Mater. Res. 32 (2017) 497–511.
[17] M.F. Slim, A. Alhussein, F. Sanchette, B. Guelorget, M. François, An enhanced formulation to determine Young's and shear moduli of thin films by means of Impulse Excitation Technique, Thin Solid Films 631 (2017) 172–179.
[18] M. Alfano, G. Di Girolamo, L. Pagnotta, D. Sun, Processing, microstructure and mechanical properties of air plasma-sprayed ceria–yttria Co-stabilized zirconia coatings, Strain 46 (2010) 409–418.
[19] M. Yamaguchi, J. Bernhardt, K. Faerstein, D. Shtansky, Y. Bando, I.S. Golovin, H.-R. Sinning, D. Golberg, Fabrication and characteristics of melt-spun Al ribbons reinforced with nano/micro-BN phases, Acta Mater. 61 (2013) 7604–7615.
[20] H.-R. Sinning, G. Vidrich, W. Riehemann, Mechanical spectroscopy of nanoparticle reinforced, electrodeposited ultrafine grained nickel, Acta Mater. 59 (2011) 4504–4510.
[21] H.-R. Sinning, Internal-friction peaks of hydrogen in amorphous and crystalline $Co_{33}Zr_{67}$, J. Phys. Condens. Matter 3 (1991) 2005–2020.
[22] U. Harms, L. Kempen, H. Neuhäuser, Influence of stress in thin film modulus measurements by the vibrating reed technique, Thin Solid Films 323 (1998) 153–157.
[23] R. Whiting, M.A. Angadi, S. Tripathi, Evaluation of elastic moduli in thin-film/substrate systems by the two-layer vibrating reed method, Mater. Sci. Eng. B 30 (1995) 35–38.
[24] S. Amadori, E.G. Campari, A.L. Fiorini, R. Montanari, L. Pasquini, L. Savini, E. Bonetti, Automated resonant vibrating-reed analyzer apparatus for a non-destructive characterization of materials for industrial applications, Mater. Sci. Eng. A 442 (2006) 543–546.
[25] S. Timoshenko, Vibration Problems in Engineering, D. van Nostrand Company, 1937.
[26] T. Fiedler, R. Groß, J. Rösler, M. Bäker, Damage mechanisms of metallic HVOF-coatings for high heat flux application, Surf. Coat. Technol. 316 (2017) 219–225.
[27] T. Fiedler, J. Schloesser, J. Rösler, M. Bäker, Development of a thermal-barrier coating-system for rocket combustion chambers, in: 6th European Conference for Aeronautics and Space Sciences, 2015.
[28] M. Bäker, T. Fiedler, J. Rösler, Stress evolution in thermal barrier coatings for rocket engine applications, Mech. Adv. Mater. Modern Process. 1 (5) (2015) 1–10.

[29] T. Fiedler, M. Bäker, J. Rösler, Large heat flux exposure of metallic coatings for rocket engine applications, Surf. Coat. Technol. 332 (2017) 30–39.
[30] [30a] T. Fiedler, H.-R. Sinning, J. Rösler, M. Bäker, Temperature dependent mechanical properties of metallic HVOF coatings, Surf. Coat. Technol. 349 (2018) 32–36.
[31] N. Rösemann, K. Ortner, J. Petersen, T. Schadow, M. Bäker, G. Bräuer, J. Rösler, Influence of bias voltage and oxygen flow rate on morphology and crystallographic properties of gas flow sputtered zirconia coatings, Surf. Coat. Technol. 276 (2015) 668–676.
[32] N. Rösemann, K. Ortner, J. Petersen, M. Stöwer, M. Bäker, G. Bräuer, J. Rösler, Influence of substrate temperature on morphology and behavior under cyclic thermal load of gas flow sputtered zirconia coatings, Surf. Coat. Technol. 324 (2017) 7–17.
[33] N. Rösemann, Microstructure of gas flow sputtered thermal barrier coatings: influence of bias voltage, Surf. Coat. Technol. 332 (2017) 22–29.
[34] N. Rösemann, K. Ortner, M. Bäker, J. Petersen, G. Bräuer, J. Rösler, Influence of the oxygen flow rate on gas flow sputtered thermal barrier coatings, J. Ceram. Sci. Technol. 9 (2017) 29–36.
[35] P.G. Bordoni, Metodo elettroacustico per ricerche sperimentali sulla elasticità. Il Nuovo Cimento, vol. 4, 1947, pp. 177–200;
[30b] T. Fiedler, J. Rösler, M. Bäker, Development of a CuNiCrAl bond coat for thermal barrier coatings in rocket combustion chambers, J. Therm. Spray Technol. 24 (2015) 1480–1486.
[37] T. Fiedler, T. Fedorova, J. Rösler, M. Bäker, Design of a nickel-based bond-coat alloy for thermal barrier coatings on copper substrates, Metals 4 (2014) 503–518.
[38] S.M. Han, H. Benaroya, T. Wei, Dynamics of transversely vibrating beams using four engineering theories, J. Sound Vib. 225 (5) (1999) 935–988.
[39] H. Si, TetGen, a delaunay-based quality tetrahedral mesh generator, ACM Trans. Math Software 41 (2015).
[40] Abaqus Analysis User's Manual (6.12), Dassault Systèmes, 2012.
[41] J. Baur, A. Kulik, Optimal sample shape for internal friction measurements using a dual cantilevered beam, J. Appl. Phys. 58 (1985) 1489–1492.
[42] T.A. Taylor, D.F. Bettridge, Development of alloyed and dispersion-strengthened MCrAlY coatings, Surf. Coat. Technol. 86–87 (1996) 9–14.
[43] W.P. Mason, Physical Acoustics and the Properties of Solids, D. van Nostrand Company, 1958.
[44] N.N. Greenwood, A. Earnshaw, Chemie der Elemente, VCH Verlagsgesellschaft, 1990.
[45] F. Tang, J.M. Schoenung, Evolution of Young's modulus of air plasma sprayed yttria-stabilized zirconia in thermally cycled thermal barrier coatings, Scr. Mater. 54 (2006) 1587–1592.
[46] C. Held, Mechanische Eigenschaften von EB-PVD ZrO2 Warmedämmschichten, Friedrich-Alexander-Universität Erlangen-Nürnberg, 2014.
[47] A. Rico, J. Gómez-García, C.J. Múnez, P. Poza, V. Utrilla, Mechanical properties of thermal barrier coatings after isothermal oxidation.: Depth sensing indentation analysis, Surf. Coat. Technol. 203 (2009) 2307–2314.
[48] B.K. Jang, H. Matsubara, Influence of rotation speed on microstructure and thermal conductivity of nano-porous zirconia layers fabricated by EB-PVD, Scr. Mater. 52 (2005) 553–558.
[49] N. Zotov, M. Bartsch, G. Eggeler, Thermal barrier coating systems — analysis of nanoindentation curves, Surf. Coat. Technol. 203 (2009) 2064–2072.
[50] R.G. Wellman, A. Dyer, J.R. Nicholls, Nano and Micro indentation studies of bulk zirconia and EB PVD TBCs, Surf. Coat. Technol. 176 (2004) 253–260.
[51] A.P. Jackson, J.F.V. Vincent, R.M. Turner, The mechanical design of nacre, Proc. R. Soc. Lond. B 234 (1277) (1988).